LETTERS

Novel mutant-selective EGFR kinase inhibitors against EGFR T790M

Wenjun Zhou[1,2]*, Dalia Ercan[3,4]*, Liang Chen[3,4]*, Cai-Hong Yun[1,2]*, Danan Li[3,4], Marzia Capelletti[3,4], Alexis B. Cortot[3,4], Lucian Chirieac[5], Roxana E. Iacob[6,7], Robert Padera[5], John R. Engen[6,7], Kwok-Kin Wong[3,4,8,9], Michael J. Eck[1,2], Nathanael S. Gray[1,2] & Pasi A. Jänne[3,4,8]

The clinical efficacy of epidermal growth factor receptor (EGFR) kinase inhibitors in *EGFR*-mutant non-small-cell lung cancer (NSCLC) is limited by the development of drug-resistance mutations, including the gatekeeper T790M mutation[1–3]. Strategies targeting EGFR T790M with irreversible inhibitors have had limited success and are associated with toxicity due to concurrent inhibition of wild-type EGFR[4,5]. All current EGFR inhibitors possess a structurally related quinazoline-based core scaffold and were identified as ATP-competitive inhibitors of wild-type EGFR. Here we identify a covalent pyrimidine EGFR inhibitor by screening an irreversible kinase inhibitor library specifically against EGFR T790M. These agents are 30- to 100-fold more potent against EGFR T790M, and up to 100-fold less potent against wild-type EGFR, than quinazoline-based EGFR inhibitors *in vitro*. They are also effective in murine models of lung cancer driven by EGFR T790M. Co-crystallization studies reveal a structural basis for the increased potency and mutant selectivity of these agents. These mutant-selective irreversible EGFR kinase inhibitors may be clinically more effective and better tolerated than quinazoline-based inhibitors. Our findings demonstrate that functional pharmacological screens against clinically important mutant kinases represent a powerful strategy to identify new classes of mutant-selective kinase inhibitors.

EGFR kinase inhibitors, gefitinib and erlotinib, are effective clinical therapies for NSCLCs that harbour activating mutations in the *EGFR* kinase domain[1,6]. The most common *EGFR* mutations, L858R and delE746_A750, impart both an increased affinity for gefitinib or erlotinib and a decreased affinity for ATP relative to wild-type (WT) EGFR[7,8]. The clinical efficacy of gefitinib or erlotinib is, however, ultimately limited by the development of acquired drug resistance such as by mutation of the gatekeeper T790 residue (T790M), which is detected in 50% of clinically resistant patients[2,3]. Unlike the analogous T315I mutation in ABL, which introduces a steric impediment for imatinib binding, EGFR T790M only modestly affects gefitinib binding. However, more importantly, it restores the affinity for ATP, similar to that of WT EGFR[9].

Most EGFR inhibitors are based on a 4-anilinoquinazoline core scaffold and were initially identified as ATP-competitive inhibitors of WT EGFR. They include irreversible inhibitors that, unlike gefitinib, contain an electrophilic functionality that undergoes a Michael addition reaction with a conserved cysteine residue present in EGFR (Cys 797). The covalent nature of these compounds allows them to achieve greater occupancy of the ATP site relative to reversible inhibitors, thus providing the ability to inhibit EGFR T790M in preclinical models, despite the increased ATP affinity conferred by this secondary mutation[4,10,11]. However, all current irreversible inhibitors are less potent in cell-line models harbouring *EGFR* T790M than those with an *EGFR*-activating mutation alone (Supplementary Fig. 1) and, at clinically achievable concentrations, these agents do not inhibit EGFR T790M *in vitro*[10–13]. Because the ATP affinity of EGFR T790M is similar to WT EGFR, the concentration of quinazoline-based EGFR inhibitors required to inhibit EGFR T790M will also effectively inhibit WT EGFR. In patients, this concurrent inhibition of WT EGFR results in skin rash and diarrhoea, and limits the ability to achieve plasma concentrations sufficient to inhibit EGFR T790M. Consequently, the clinical efficacy of the irreversible EGFR inhibitors CI-1033, HKI-272 and PF00299804 has been limited, especially in patients with gefitinib- or erlotinib-resistant NSCLC, and the dose-limiting toxicity has been diarrhoea and skin rash[5,14,15].

We hypothesized that the anilinoquinazoline scaffold may not be the most potent or specific for inhibiting EGFR T790M because it relies on the small size and hydrogen bonding interactions with the gatekeeper threonine of WT EGFR. We prepared a focused library of common kinase inhibitor core scaffolds where one of the side chains was modified with an acrylamide group at a position that molecular modelling predicted to react with Cys 797. This library was screened for compounds that could inhibit the growth of both gefitinib-resistant (PC9GR; delE746_A750/T790M) and -sensitive (PC9; delE746_A750) cell lines but were not toxic up to 10 μM against A549 (*KRAS* mutant) or H3122 (*EML4-ALK*) cells. We compared our findings with both reversible (gefitinib) and irreversible EGFR inhibitors (CL-387,785 and HKI-272). Three closely related pyrimidines, WZ3146, WZ4002 and WZ8040, were identified from the screen that possessed up to a 300-fold lower half-maximum inhibitory concentration (IC_{50}) against the PC9GR cells compared with clinical-stage inhibitors such as HKI-272 (Fig. 1a, b and Supplementary Table 1). We observed a similar increased potency of the WZ compounds in the H1975 (L858R/T790M) cell line and in Ba/F3 cells harbouring *EGFR* T790M (Fig. 1b and Supplementary Tables 1 and 2). The increased cellular potency correlated with inhibition of EGFR, AKT and ERK1/2 phosphorylation in NSCLC cell lines (Fig. 1c and Supplementary Fig. 2) and with the more potent inhibition of EGFR phosphorylation by WZ4002 in NIH-3T3 cells expressing different *EGFR* T790M mutant alleles (Fig. 1d and Supplementary Fig. 3). The profile against ERBB2 was markedly different: the WZ compounds were less potent than CL-387,785 or HKI-272 (Supplementary Tables 1 and 2) and did not inhibit ERBB2

[1]Department of Cancer Biology, [2]Department of Biological Chemistry and Molecular Pharmacology, [3]Lowe Center for Thoracic Oncology, [4]Department of Medical Oncology, Dana-Farber Cancer Institute, 44 Binney Street, Boston, Massachusetts 02115, USA. [5]Department of Pathology, Brigham and Women's Hospital, Boston, Massachusetts 02115, USA. [6]The Barnett Institute of Chemical & Biological Analysis, [7]Department of Chemistry and Chemical Biology, Northeastern University, Boston, Massachusetts 02115, USA. [8]Department of Medicine, Brigham and Women's Hospital and Harvard Medical School, Boston, Massachusetts 02115, USA. [9]Ludwig Center at Dana-Farber/Harvard Cancer Center, Boston, Massachusetts 02115, USA.
*These authors contributed equally to this work.

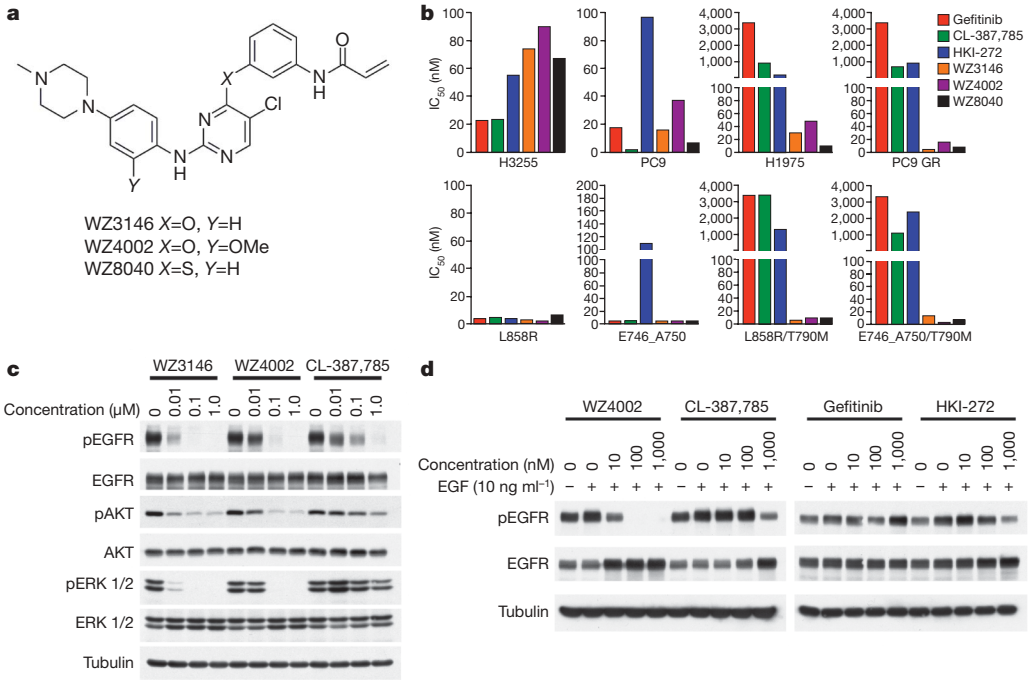

Figure 1 | WZ4002, WZ3146 and WZ8040 are novel EGFR inhibitors, suppress the growth of *EGFR*-T790M-containing cell lines and inhibit EGFR phosphorylation. **a**, Chemical structures of the WZ compounds. **b**, IC_{50} values for NSCLC cell lines (top) and Ba/F3 cells (bottom), with genotypes corresponding to the NSCLC cell lines, treated with indicated drugs. Growth was assessed using the MTS (3-(4,5-dimethylthiazol-2-yl)-5-(3-carboxymethoxyphenyl)-2-(4-sulfophenyl)-2H-tetrazolium) survival assay. **c**, Comparison of WZ3146, WZ4002 and CL-387,785 on EGFR signalling in PC9 GR cells. The cells were treated with the indicated concentrations of each drug for 16 h. Cell extracts were immunoblotted to detect the indicated proteins. **d**, Comparison of EGFR inhibitors on EGFR phosphorylation in 3T3 cells expressing del E746_A750/T90M. The cells were treated with indicated concentrations of each drug for 16 h and stimulated with EGF (10 ng ml^{-1}) 15 min before lysis. Cell extracts were immunoblotted to detect the indicated proteins.

phosphorylation in 3T3 cells expressing the ERBB2 gatekeeper (T798I) mutation (data not shown). Analysis of recombinant EGFR T790M kinase incubated with WZ3146 by electrospray mass spectrometry revealed stoichiometric addition of one inhibitor molecule to the protein. Analysis of a pepsin digest of the modified protein by tandem mass spectrometry identified Cys 797 as the site of modification, thus verifying covalent bond formation between WZ3146 and EGFR (Supplementary Fig. 4).

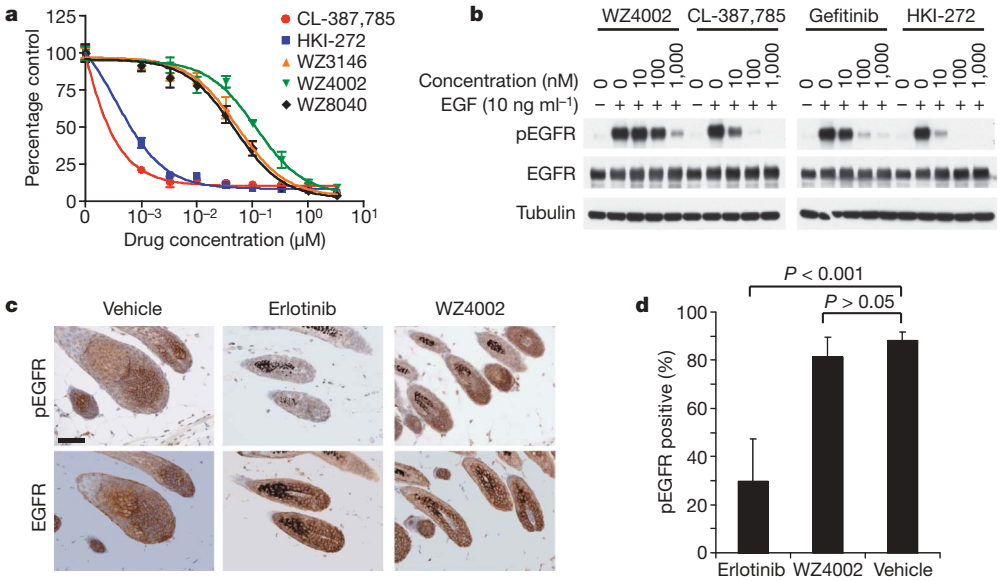

Figure 2 | WZ4002 is less potent than quinazoline EGFR inhibitors against WT EGFR *in vitro* and *in vivo*. **a**, EGFR vIII Ba/F3 cells treated with WZ or quinazoline EGFR inhibitors. The mean ($n = 6$) and standard deviation is plotted for each drug and concentration. **b**, Comparison of EGFR inhibitors on EGFR phosphorylation in 3T3 cells expressing WT EGFR. The cells were treated with indicated concentrations of each drug for 16 h and stimulated with EGF (10 ng ml^{-1}) 15 min before lysis. Cell extracts were immunoblotted to detect the indicated proteins. **c**, Immunohistochemical analysis of hair bulb from erlotinib- or WZ4002-treated mice using EGFR and pY1173 EGFR. Only treatment with erlotinib results in significant inhibition of EGFR phosphorylation. Scale bar, 50 μm. **d**, Quantification of frequency of phospho-EGFR staining from vehicle- ($n = 3$), erlotinib- ($n = 3$) and WZ4002- ($n = 2$) treated mice. The means and standard deviations are plotted for drug treatment.

We profiled WZ3146 and WZ4002 against a panel of 400 kinases using the Ambit kinome screening platform (Supplementary Table 3 and Supplementary Fig. 5). For WZ4002, kinases that exhibited greater than 95% inhibition relative to the dimethylsulphoxide control (Ambit score <5) at 10 μM were selected for measurement of their dissociation constants (Supplementary Table 3). In addition to EGFR, we observed potent inhibition of several of the ten kinases that possess a cysteine at the same position as EGFR, including a subset of the TEC-family kinases (Supplementary Fig. 6). Cross-reactivity with BMX has been reported for irreversible quinazoline-derived EGFR inhibitors[16]. To confirm whether the observed binding activity translated into cellular inhibition, WZ4002 and WZ3146 were profiled against Ba/F3 cells transformed with TEL fusions of BMX, BLK, JAK2 and JAK3. WZ4002, which possesses an ortho-methoxy group at the C2-aniline substituent, is more selective for EGFR than WZ3146 (Supplementary Table 4).

We next determined whether the increased potency of the WZ compounds against mutant EGFR also applied to WT EGFR. We used *EGFR* WT HN11 cells[17] and Ba/F3 cells harbouring the *EGFR* vIII mutation, which contains a WT kinase domain (Fig. 2a and Supplementary Table 2). These compounds were 3- to 100-fold less potent, with WZ4002 being least potent, than CL-387,785 and HKI-272 at inhibiting the growth of the *EGFR* WT cells. Furthermore, WZ4002 was 100-fold less effective at inhibiting phosphorylation of WT EGFR than the quinazoline inhibitors (Fig. 2b). Similarly, WZ4002 inhibited EGFR kinase activity of recombinant L858R/T790M protein more potently than that of WT EGFR, whereas the opposite was observed with HKI-272 and gefitinib (Supplementary Fig. 7a, b).

To understand better the potency and relative selectivity for EGFR T790M over WT EGFR, we determined the crystal structure of WZ4002 in complex with EGFR T790M (Fig. 3a, b, Supplementary Fig. 8 and Supplementary Table 5). The compound binds within the ATP-binding cleft of the enzyme, forming the expected covalent bond with Cys 797. As expected based upon co-structures of related pyrimidine-derived inhibitors with CDK2 (ref. 18), JNK1 (ref. 19) and FAK[20], the anilinopyrimidine core of WZ4002 forms a bidentate hydrogen bonding interaction with the 'hinge' residue Met 793 (Fig. 3b). The chlorine substituent on the pyrimidine ring contacts the mutant gatekeeper residue, Met 790. The hydrophobicity conferred by this mutation likely contributes to the potency of these compounds against the T790M mutant. The aniline ring forms a hydrophobic interaction with the α-carbon of Gly 796 and its methoxy substituent extends towards Leu 792 and Pro 794 in the hinge region. The greater selectivity of the WZ4002 compound likely derives from the fact that both JAK3 and TEC-family kinases have a bulkier residue (tyrosine in JAK3, phenylalanine in TEC-family kinases) in the position of Leu 792, which would be expected to interfere sterically with the methoxy group in WZ4002. The reactive acrylamide moeity and the linking phenyl ring comprise the other arm of the inhibitor. The 'linker' phenyl ring lies roughly perpendicular to the pyrimidine core; this orientation juxtaposes the acrylamide with the thiol of Cys 797 for covalent bond formation (Fig. 3b).

We further determined whether WZ4002 is effective *in vivo* by using mouse lung cancer models harbouring either *EGFR* L858R/T790M or Del E746_A750/T790M. We chose WZ4002 for the *in vivo* studies because *in vitro* it was least potent against WT EGFR and other cysteine-containing kinases (Supplementary Tables 2 and 4) but was effective against EGFR T790M. A pharmacokinetic study was performed to determine the achievable plasma concentration (429 ng ml^{-1}), half-life (2.5 h) and the oral bioavailability (24%) of WZ4002 (Supplementary Tables 6–8). In a pharmacodynamic study, WZ4002 effectively inhibited EGFR, AKT and ERK1/2 phosphorylation (Fig. 4a), which was associated with a significant increase in TdT-mediated dUTP nick-end labelling (TUNEL)-positive and a significant decrease in Ki67-positive cells compared with mice treated by vehicle alone (Fig. 4b, c). To evaluate whether WZ4002 imparted a differential effect on WT EGFR *in vivo*, we evaluated EGFR phosphorylation in the hair bulb from mouse skin after treatment with either erlotinib or WZ4002

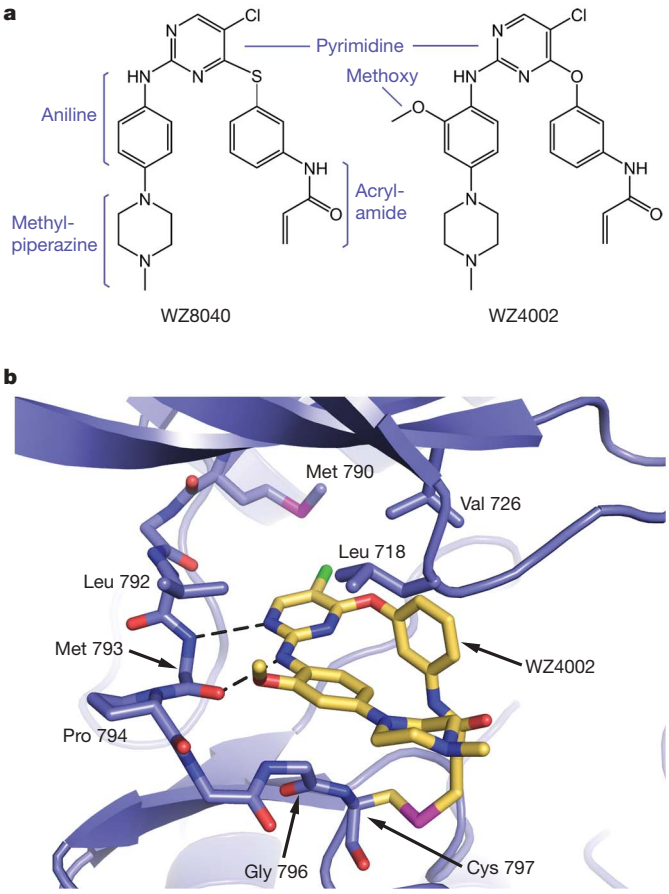

Figure 3 | Crystal structure of WZ4002 bound to EGFR T790M. **a**, Chemical structures of WZ8040 and WZ4002 are shown schematically in a manner resembling the conformation adopted in complex with the kinase. **b**, Crystal structure of WZ4002 in complex with EGFR T790M mutant (PDB ID 3IKA). WZ4002 binds the active conformation of the kinase, with both the regulatory C-helix and the 'DFG' segment of the activation loop in their inward, active positions. The EGFR kinase is shown in a ribbon representation (blue) with the bound inhibitor in yellow. Side-chain and main-chain atoms are shown for selected residues that contact the compound. Expected hydrogen bonds to the backbone amide and carbonyl atoms of Met 793 are indicated by dashed lines. Note also the covalent bond with Cys 797. The structure was refined to a crystallographic *R* value of 21.3% (R_{free} = 25.4%) with data extending to 2.9-Å resolution (see Methods for further crystallographic details).

(Fig. 2c, d). Only erlotinib significantly inhibited EGFR phosphorylation in the hair bulb. In a 2-week efficacy study, WZ4002 treatment resulted in significant tumour regressions compared with vehicle alone in both T790M-containing murine models (Fig. 4d, e and Supplementary Fig. 9). Histological evaluation of the lungs after treatment confirmed significant resolution of the tumour nodules, with only a few small residual nodules and nodule remnants that had evidence of treatment effect with decreased cellularity and increased fibrosis consistent with remodelling/scarring (Fig. 4f). There were no signs of overt toxicity compared with mice treated by vehicle alone during the study as assessed by changes in weight (data not shown), serum creatine and total white blood cell count (Supplementary Fig. 10).

Our studies identify a novel structural class of EGFR kinase inhibitors that are effective *in vitro* and in *in vivo* models harbouring the *EGFR* T790M mutation. Given the marked activity in models with established *EGFR* T790M, we determined whether WZ4002 treatment could also prevent the development of *EGFR* T790M using *in vitro* models harbouring *EGFR*-activating mutations. Unlike with gefitinib or HKI-272, which when used at their achievable plasma concentrations lead to development of *EGFR* T790M *in vitro*[13,21,22],

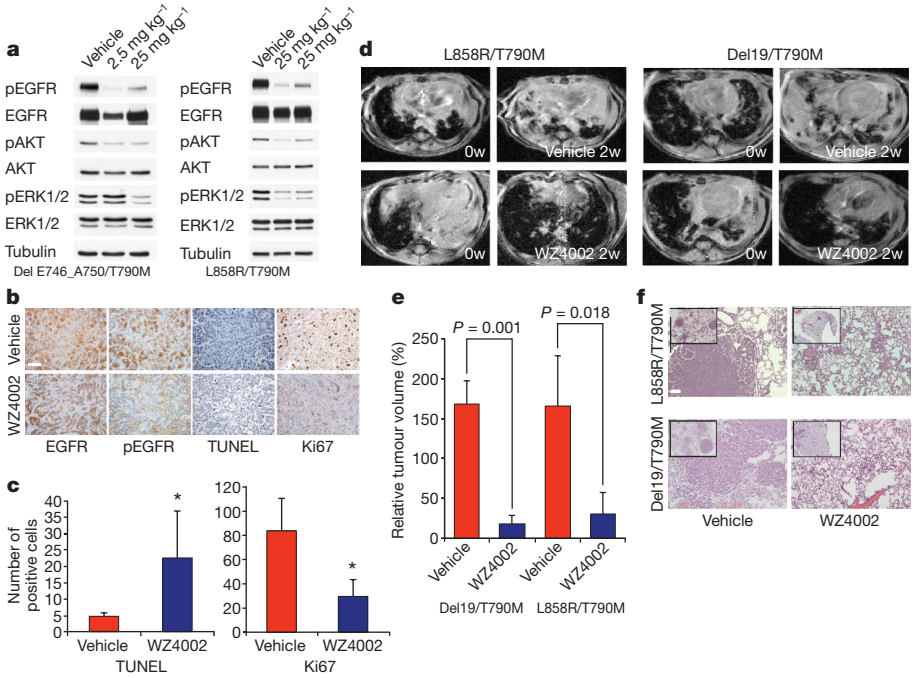

Figure 4 | WZ4002 inhibits EGFR phosphorylation and induces significant tumour regression in murine models of *EGFR* T790M. **a**, Two doses separated by 16 h of WZ4002 (2.5 mg kg^{-1} or 25 mg kg^{-1}) or vehicle were administered to EGFR delE746_A750/T790M or L858R/T790M mice with MRI-confirmed tumours. The mice were killed, the lungs isolated, grossly dissected and subjected to cell lysis. Cell extracts were immunoblotted to detect the indicated proteins. **b**, Immunohistochemical analyses of tumours from EGFR delE746_A750/T790M mice from **a** using indicated antibodies. Scale bar, 50 μm. **c**, Quantification of TUNEL- and Ki67-positive cells from tumour nodules ($n = 4$) from vehicle- and WZ4002-treated mice. The means and standard deviations are plotted. *, $P < 0.05$. **d**, MRI images of vehicle- or WZ4002-treated mice at baseline (0 weeks: 0w) and after 2 weeks (2w) of treatment. **e**, Quantification of the relative tumour volume from MRI images from vehicle-treated mice (E746_A750/T790M ($n = 3$); L858R/T790M ($n = 4$)), and WZ4002-treated L858R/T790M ($n = 3$) and E746_A750/T790M ($n = 3$) mice. The means and standard deviations are plotted. **f**, Tumours from vehicle- and WZ4002-treated mice stained with haematoxylin and eosin. Low-power view (inset) demonstrates near-complete resolution of tumours in the WZ4002-treated mice. Scale bar, 100 μm.

we were unable to isolate any *EGFR*-T790M-containing clones from WZ4002-treated Ba/F3 or PC9 NSCLC cells (Supplementary Table 9). These findings suggest that WZ4002 could also be used as initial therapy for patients with *EGFR*-mutant NSCLC and may ultimately lead to a longer time to disease progression than currently achieved with gefitinib[1].

Our crystallographic studies provide insight into why WZ4002 is so much more effective against L858R/T790M than HKI-272. Although both share the irreversible component, the anilinopyrimidine scaffold of WZ4002 is an intrinsically better fit for the mutant gatekeeper methionine (Supplementary Fig. 11). To test this hypothesis further, we prepared WZ4003, a reversible analogue of WZ4002 that is non-reactive towards Cys 797. WZ4003 binds to the L858R/T790M mutant 100-fold more tightly than it does to the WT EGFR (Supplementary Table 10), confirming that the scaffold per se is indeed specific for the mutant kinase. Importantly, the WZ compounds rely on covalent bond formation for potent cellular inhibition, as evidenced by the 100-fold increase in the IC_{50} of WZ4002 against the *EGFR* C797S mutants and by the significantly reduced cellular IC_{50} of WZ4003 against T790M containing Ba/F3 cells (Supplementary Table 2). These observations highlight the importance of using a library of irreversible kinase inhibitors, as WZ4003 would not have been identified in the initial cellular screen.

Mutations, including those at the gatekeeper residue, are a common mechanism of drug resistance to kinase inhibitors. The current approach, using a cellular screen expressing the mutant kinase of interest, can be applied to identify novel agents specifically against drug resistance or oncogenic mutations implicated in human cancers. Such agents may truly be cancer selective, clinically more potent and less toxic than those that also concurrently inhibit the WT kinase. The agents described here are unique in that they inhibit both the drug sensitizing and resistance mutations but are selective against WT EGFR[23–25]. Further studies are needed to determine whether this class of EGFR inhibitors will be clinically effective in patients with *EGFR*-mutant cancers harbouring *EGFR*-T790M-mediated acquired drug resistance.

METHODS SUMMARY

Kinase inhibitors. Gefitinib, CL-387,785 and HKI-272 were obtained from commercial sources. The WZ compounds were synthesized using a four-step chemical synthesis that is described in detail in the Supplementary Methods. The final products were verified by ^{1}H nuclear magnetic resonance and liquid chromatography–mass spectrometry.

Cell lines. *EGFR* wild-type and mutant NSCLC, Ba/F3 cells and NIH-3T3 cells were cultured as previously described[10]. The PC9GR4 cells were generated as previously described and verified to contain EGFR delE746_A750/T790M by direct sequencing[21]. Cell proliferation and growth assays were performed using a colorimetric assay as previously described[26]. Site-directed mutagenesis was performed using the Quick Change Site-Directed Mutagenesis kit (Stratagene) according to the manufacturer's instructions.

EGFR kinase assays. *In vitro* inhibitory enzyme kinetic assays using recombinant EGFR L858R/T790M and WT protein and were performed using the ATP/NADH coupled assay system in a 96-well format as previously described[7].

Crystal structure determination and refinement. The structure of WZ4002 in complex with EGFR T790M was determined as previously described[9].

Mouse studies. All studies involving mice were approved by the Dana-Farber Cancer Institute Animal Care and Use Committee. EGFR-TL (T790M/L858R) mice were generated as previously described[4]. EGFR exon 19 deletion-T790M (TD)-inducible bitransgenic mice were similarly generated and characterized. Mice were treated either with vehicle (10% 1-methyl-2-pyrrolidinone:90% PEG-300) alone or WZ4002 at 25 mg kg^{-1} gavage daily. This was followed by magnetic resonance imaging (MRI) scanning as previously described[4,27]. Histology, immunohistochemistry and immunoblotting analyses were performed according to standard protocols, as previously described[4,10].

Generation of drug-resistant cells. *N*-ethyl-*N*-nitrosourea mutagenesis was performed using *EGFR* L858R and DelE746_A750 Ba/F3 cells as previously described[28]. Treated cells were expanded in 100 nM WZ4002, 1 μM WZ4002,

200 nM HKI-272 or 1 μM gefitnib. Resistant clones were isolated and further characterized.

Received 16 April; accepted 29 October 2009.

1. Mok, T. S. *et al.* Gefitinib or carboplatin-paclitaxel in pulmonary adenocarcinoma. *N. Engl. J. Med.* **361,** 947–957 (2009).
2. Pao, W. *et al.* Acquired resistance of lung adenocarcinomas to gefitinib or erlotinib is associated with a second mutation in the EGFR kinase domain. *PLoS Med.* **2,** 1–11 (2005).
3. Kobayashi, S. *et al.* EGFR mutation and resistance of non-small-cell lung cancer to gefitinib. *N. Engl. J. Med.* **352,** 786–792 (2005).
4. Li, D. *et al.* Bronchial and peripheral murine lung carcinomas induced by T790M–L858R mutant EGFR respond to HKI-272 and rapamycin combination therapy. *Cancer Cell* **12,** 81–93 (2007).
5. Besse, B. *et al.* Neratinib (HKI-272), an irreversible pan-ErbB receptor tyrosine kinase inhibitor: preliminary results of a phase 2 trial in patients with advanced non-small cell lung cancer. *Eur. J. Cancer Suppl.* **6,** 64, abstr. 203 (2008).
6. Rosell, R. *et al.* Screening for epidermal growth factor receptor mutations in lung cancer. *N. Engl. J. Med.* **361,** 958–967 (2009).
7. Yun, C. H. *et al.* Structures of lung cancer-derived EGFR mutants and inhibitor complexes: mechanism of activation and insights into differential inhibitor sensitivity. *Cancer Cell* **11,** 217–227 (2007).
8. Carey, K. D. *et al.* Kinetic analysis of epidermal growth factor receptor somatic mutant proteins shows increased sensitivity to the epidermal growth factor receptor tyrosine kinase inhibitor, erlotinib. *Cancer Res.* **66,** 8163–8171 (2006).
9. Yun, C. H. *et al.* The T790M mutation in EGFR kinase causes drug resistance by increasing the affinity for ATP. *Proc. Natl Acad. Sci. USA* **105,** 2070–2075 (2008).
10. Engelman, J. A. *et al.* PF00299804, an irreversible pan-ERBB inhibitor, is effective in lung cancer models with EGFR and ERBB2 mutations that are resistant to gefitinib. *Cancer Res.* **67,** 11924–11932 (2007).
11. Li, D. *et al.* BIBW2992, an irreversible EGFR/HER2 inhibitor highly effective in preclinical lung cancer models. *Oncogene* **27,** 4702–4711 (2008).
12. Yuza, Y. *et al.* Allele-dependent variation in the relative cellular potency of distinct EGFR inhibitors. *Cancer Biol. Ther.* **6,** 661–667 (2007).
13. Godin-Heymann, N. *et al.* The T790M 'gatekeeper' mutation in EGFR mediates resistance to low concentrations of an irreversible EGFR inhibitor. *Mol. Cancer Ther.* **7,** 874–879 (2008).
14. Janne, P. A. *et al.* Preliminary activity and safety results from a phase I clinical trial of PF-00299804, an irreversible pan-HER inhibitor, in patients (pts) with NSCLC. *J. Clin. Oncol.* 26 (Suppl.), abstr 8027 (2008).
15. Janne, P. A. *et al.* Multicenter, randomized, phase II trial of CI-1033, an irreversible pan-ERBB inhibitor, for previously treated advanced non small-cell lung cancer. *J. Clin. Oncol.* **25,** 3936–3944 (2007).
16. Hur, W. *et al.* Clinical stage EGFR inhibitors irreversibly alkylate Bmx kinase. *Bioorg. Med. Chem. Lett.* **18,** 5916–5919 (2008).
17. Yonesaka, K. *et al.* Autocrine production of amphiregulin predicts sensitivity to both gefitinib and cetuximab in EGFR wild-type cancers. *Clin. Cancer Res.* **14,** 6963–6973 (2008).
18. Breault, G. A. *et al.* Cyclin-dependent kinase 4 inhibitors as a treatment for cancer. Part 2: identification and optimisation of substituted 2,4-bis anilino pyrimidines. *Bioorg. Med. Chem. Lett.* **13,** 2961–2966 (2003).
19. Alam, M. *et al.* Synthesis and SAR of aminopyrimidines as novel c-Jun N-terminal kinase (JNK) inhibitors. *Bioorg. Med. Chem. Lett.* **17,** 3463–3467 (2007).
20. Lietha, D. & Eck, M. J. Crystal structures of the FAK kinase in complex with TAE226 and related bis-anilino pyrimidine inhibitors reveal a helical DFG conformation. *PLoS One* **3,** e3800 (2008).
21. Ogino, A. *et al.* Emergence of epidermal growth factor receptor T790M mutation during chronic exposure to gefitinib in a non small cell lung cancer cell line. *Cancer Res.* **67,** 7807–7814 (2007).
22. Engelman, J. A. *et al.* Allelic dilution obscures detection of a biologically significant resistance mutation in EGFR-amplified lung cancer. *J. Clin. Invest.* **116,** 2695–2706 (2006).
23. Tsai, J. *et al.* Discovery of a selective inhibitor of oncogenic B-Raf kinase with potent antimelanoma activity. *Proc. Natl Acad. Sci. USA* **105,** 3041–3046 (2008).
24. O'Hare, T. *et al.* SGX393 inhibits the CML mutant Bcr-AblT315I and preempts *in vitro* resistance when combined with nilotinib or dasatinib. *Proc. Natl Acad. Sci. USA* **105,** 5507–5512 (2008).
25. Gontarewicz, A. *et al.* PHA-680626 exhibits anti-proliferative and pro-apoptotic activity on imatinib-resistant chronic myeloid leukemia cell lines and primary CD34+ cells by inhibition of both Bcr-Abl tyrosine kinase and Aurora kinases. *Leuk. Res.* **32,** 1857–1865 (2008).
26. Engelman, J. A. *et al.* MET amplification leads to gefitinib resistance in lung cancer by activating ERBB3 signaling. *Science* **316,** 1039–1043 (2007).
27. Ji, H. *et al.* The impact of human EGFR kinase domain mutations on lung tumorigenesis and *in vivo* sensitivity to EGFR-targeted therapies. *Cancer Cell* **9,** 485–495 (2006).
28. Bradeen, H. A. *et al.* Comparison of imatinib mesylate, dasatinib (BMS-354825), and nilotinib (AMN107) in an *N*-ethyl-*N*-nitrosourea (ENU)-based mutagenesis screen: high efficacy of drug combinations. *Blood* **108,** 2332–2338 (2006).

Supplementary Information is linked to the online version of the paper at www.nature.com/nature.

Acknowledgements This study is supported by grants from the National Institutes of Health RO1CA11446 (P.A.J.), R01CA135257 (P.A.J.), R01CA080942 (M.J.E.), R01CA130876-02 (N.S.G.), R01CA116020 (M.J.E.), R01AG2400401 (K.-K.W.), R01 CA122794 (K.-K.W.), R01GM070590 (J.R.E.), National Cancer Institute Lung SPORE P50CA090578 (P.A.J. and K.-K.W.), the Cecily and Robert Harris Foundation (K.-K.W.), Uniting Against Lung Cancer (K.-K.W.), the Flight Attendant Medical Research Institute (K.-K.W.)., the Hazel and Samuel Bellin Research Fund (P.A.J.) and the Damon Runyon Foundation Cancer Innovation Award (N.S.G.). This work is contribution 948 from the Barnett Institute. The authors thank Sai Advantium Pharma for performing the pharmacokinetic studies.

Author Contributions W.Z., D.E., Li.C., C.-H.Y., D.L., M.C. A.B.C. designed experiments, conducted studies and analysed data. R.E.I. and J.R.E. performed and analysed the mass spectrometry studies. Lu.C. and R.P. performed the histological and immunohistochemistry analyses. M.J.E., K.-K.W., N.S.G. and P.A.J. designed the experiments, analysed data and wrote the manuscript. The Wong, Eck, Gray and Jänne laboratories contributed equally to this work.

Author Information Structural data are deposited in Protein Data Bank under accession number 3IKA. Reprints and permissions information is available at www.nature.com/reprints. The authors declare competing financial interests: details accompany the full-text HTML version of the paper at www.nature.com/nature. Correspondence and requests for materials should be addressed to N.S.G. (Nathanael_Gray@dfci.harvard.edu) or P.A.J. (pjanne@partners.org).